Synthesis, characterization, DNA interaction, and anticancer studies of novel facial tricarbonylrhenium(I) complexes with uracil-derived ligands

Shabaaz Abdullah, [a] Candace Davison, [b] Christie Jane Smit,[b] Phiwokuhle Mbatha,[a] Jo-Anne de la Mare*, [b] Irvin Noel Booysen*,[a]

[a.] School of Chemistry and Physics, University of KwaZulu-Natal, Pietermaritzburg, 3201, South Africa. E-mail: booyseni@ukzn.ac.za (INB)

[b.] Biomedical Biotechnology Research Unit, Department of Biochemistry and Microbiology, Faculty of Science, Rhodes University, PO Box 94, Grahamstown 6140, South Africa. E-mail: j.delamare@ru.ac.za (JDLM)

Details of selected experimental methodologies:

Materials and methods:

The reagents used in the research study include 5,6-diamino-1,3-dimethyluracil (urda), 2-quinolinecarboxaldehyde, bromopentacarbonylrhenium(I), pentacarbonylchlororhenium(I), calf thymus DNA, and phosphate-buffered saline. Toluene was dried over a sodium wire and stored over dried molecular sieves, while other solvents were used as obtained. Ultrapure water was collected from the Elga Purelab Option water purification system. The NMR spectra were recorded in DMSO-d_6, $CDCl_3$-d_1, or THF-d_8 and were obtained *via* a 400 MHz Bruker Avance spectrometer equipped with an autosampler. An Agilent Cary 60 instrument was used to obtain UV-Vis spectra in DMF, which was measured at a physiological temperature of 37°C. Molar extinction coefficients (ε) are reported in $M^{-1}cm^{-1}$.

The melting points were measured using a Stuart SMP3 melting point apparatus. Mass spectra of each metal complex were obtained *via* the direct injection of the samples into a Shimadzu LCMS-2020 analyser with an Electron Spray Ionisation (ESI) source, and were obtained in the positive and negative modes. A ThermoScientific Flash 2000 Organic Elemental CHNS-O Analyser was used to determine the elemental compositions of the individual metal complexes.

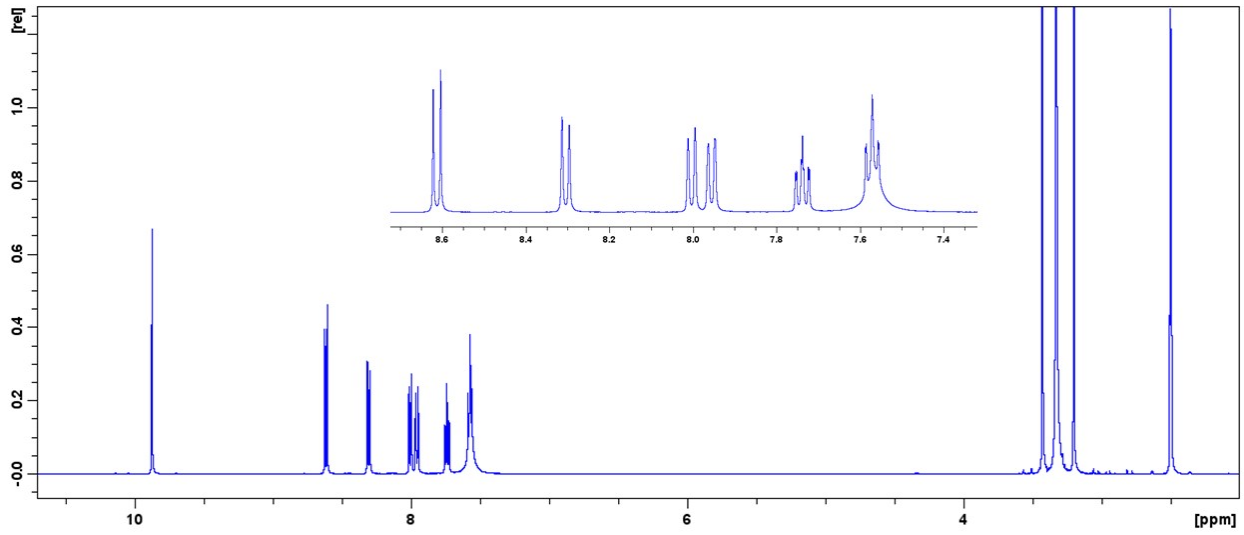

Figure S1: *^{1}H NMR spectrum of ligand urqn. Inset shows aromatic protons between 7.55-8.61 ppm.*

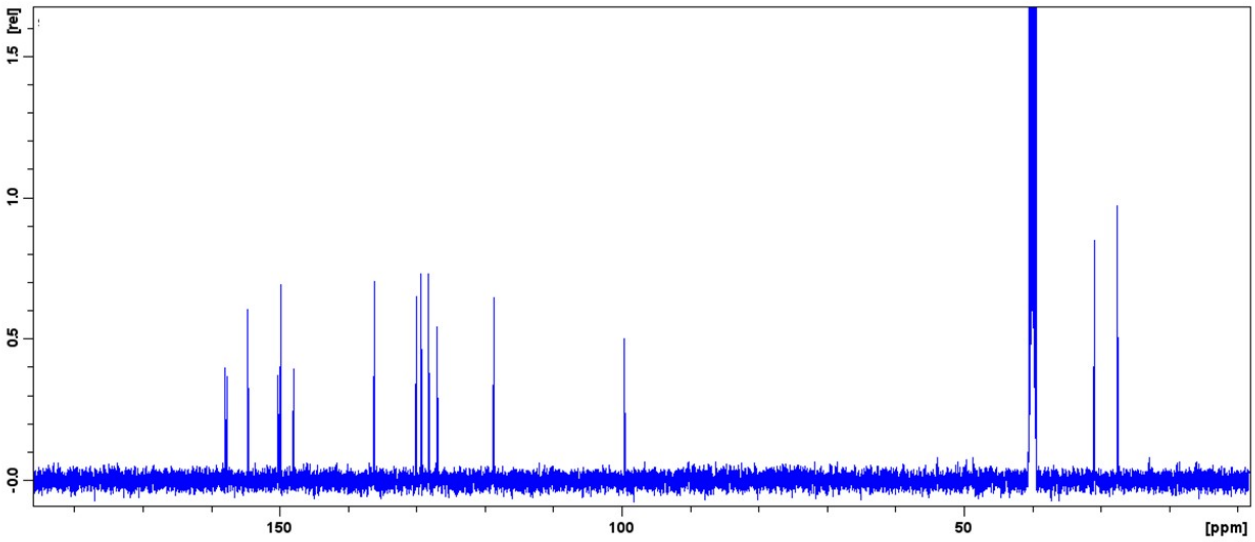

Figure S2: *^{13}C NMR spectrum of urqn.*

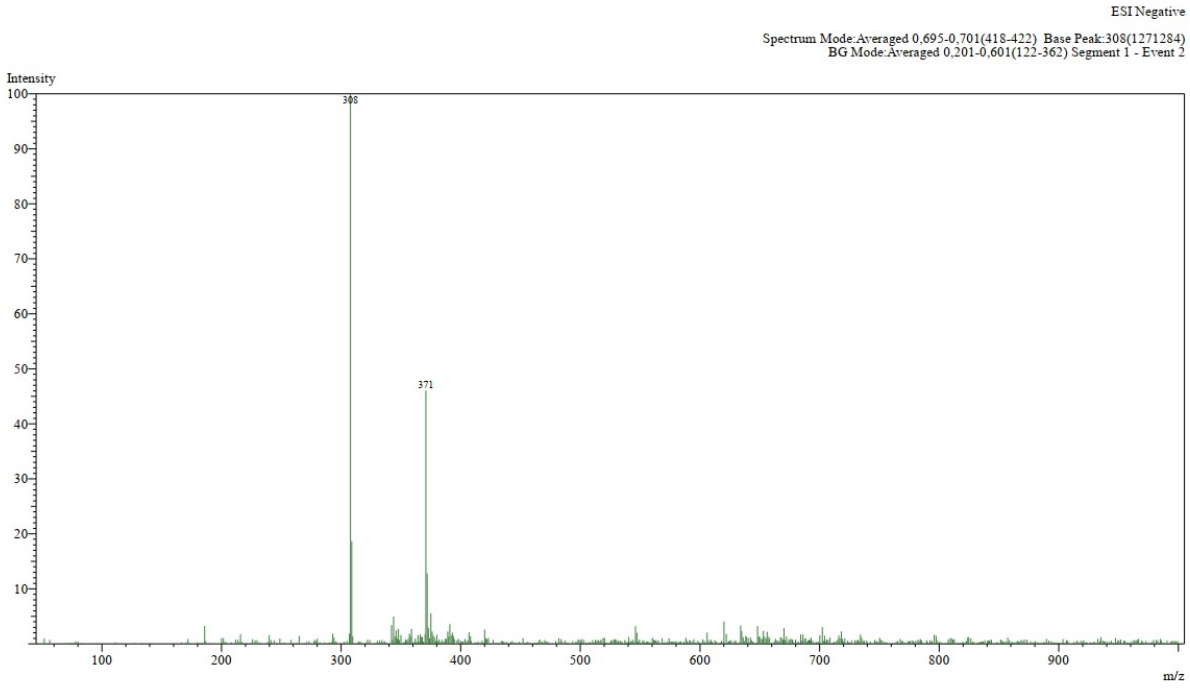

Figure S3: *Mass spectrum of urqn.*

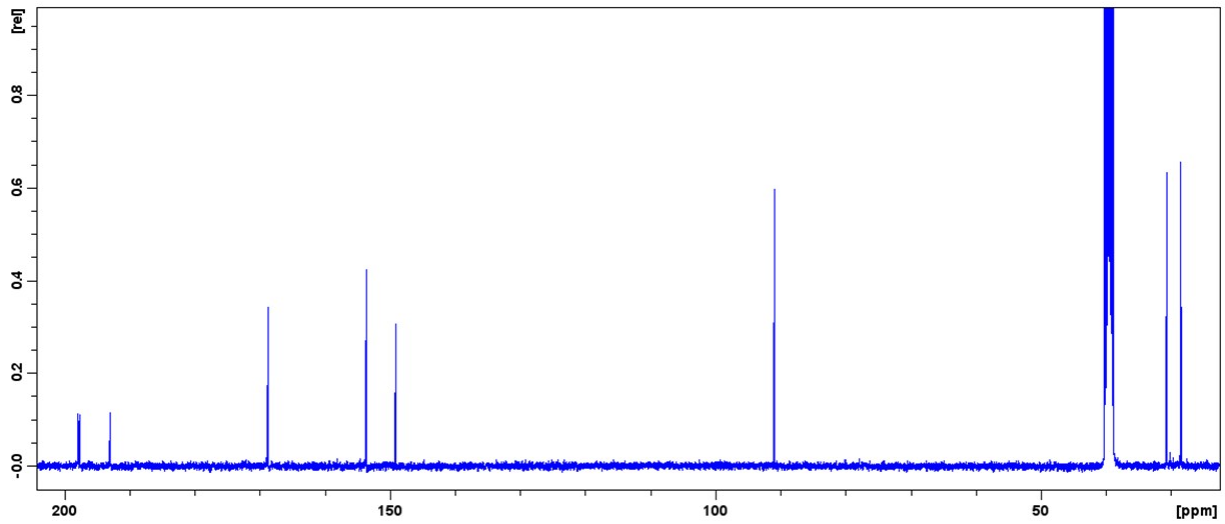

Figure S4: *^{13}C NMR spectrum of fac-[Re(CO)$_3$(urda)Cl].*

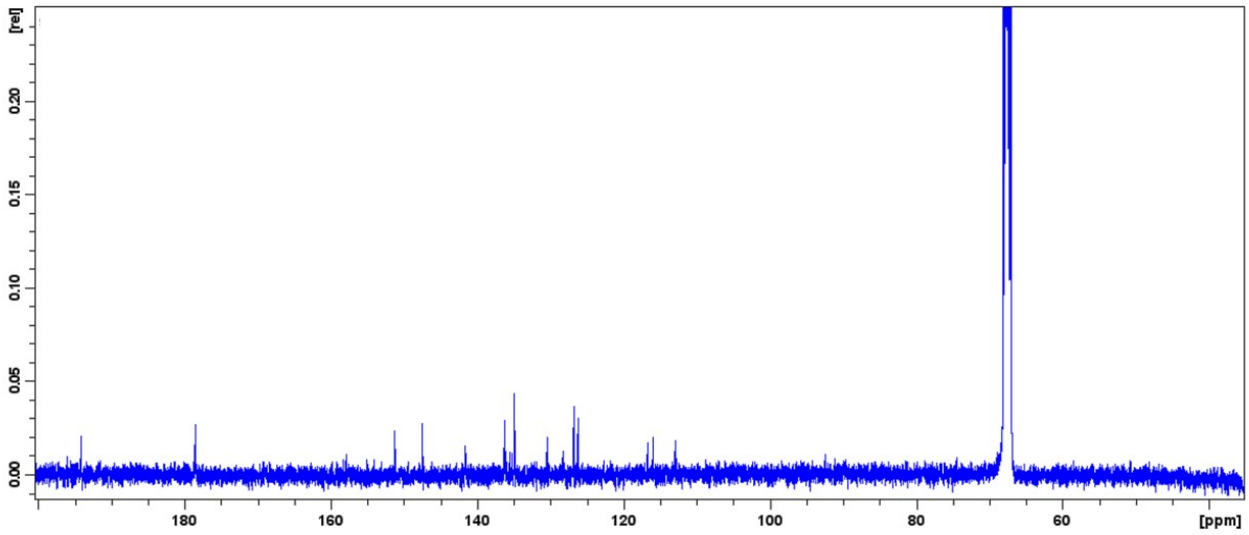

Figure S5: *^{13}C NMR spectrum of fac-[Re(CO)$_3$(uramb)Br].*

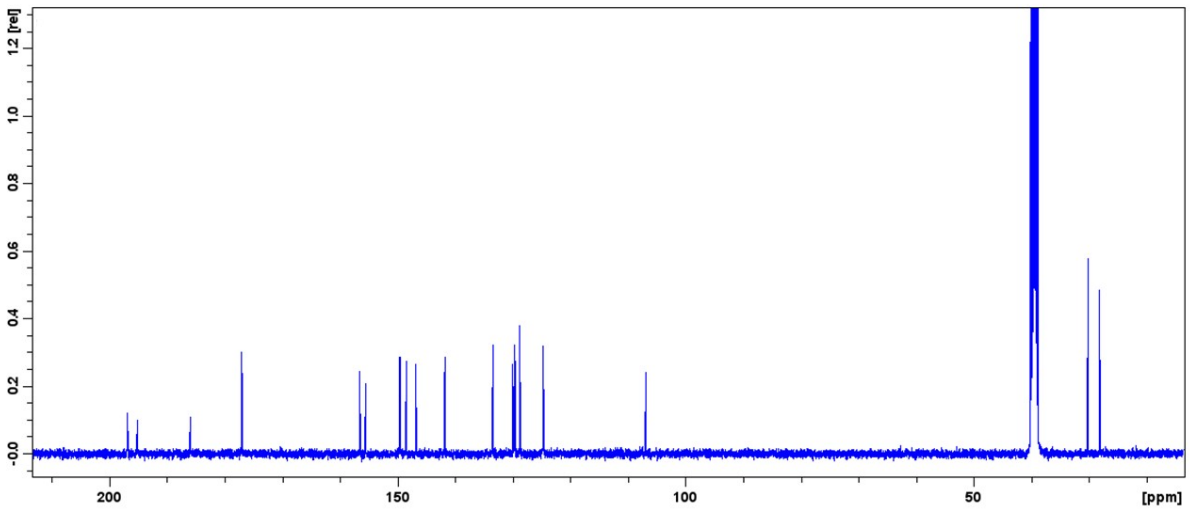

Figure S6: *^{13}C NMR spectrum of fac-[Re(CO)$_3$(urqn)Br].*

X-ray diffraction

Single crystals of **1 – 3** were used to record X-ray data on a Bruker Apex-II device equipped with an Oxford Instruments Cryojet operating at 101 K and an Incoatec microsource operating at 30 W power. The X-ray sources Mo Kα (λ = 0.71073 Å) radiation and Cu Kα (λ = 1.5406 Å) were used to collect the data at a crystal-to-detector distance of 50 mm. The following conditions were used for data collection: omega and phi scans with exposures taken at 30 W X-ray power and 0.50º frame widths using APEX2. The program SAINT was used to reduce the data using outlier rejection, scan speed scaling, as well as standard Lorentz and polarisation correction factors. A SADABS semi-empirical multi-scan absorption correction was applied to the data. All structures were solved *via* direct methods, SHELX and WinGX.[1-4] The crystal refinement details are listed in **Table S1**, while the geometrical parameters of the metal complexes are listed in **Tables S2 – S4**.

Table S1: *Crystal data and structure refinement data for **1**-**3**.*

	1	**2**	**3**
Chemical formula	$C_{26}H_{36}C_{l2}N_8O_{12}Re_2$	$C_{24}H_{31}BrN_5O_7Re$	$C_{19}H_{15}BrN_5O_5Re$
Formula weight	1095.93	767.65	659.47
Crystal system	Triclinic	Orthorhombic	Monoclinic
Space group	*P-1*	*P b c a*	$P2_1/c$
Temperature (K)	100(2) K	100(2) K	100(2) K
Unit cell dimensions			
a (Å)	10.6588(7)	18.9342(10)	15.1900(8)
b (Å)	12.0358(7)	10.1940(5)	10.7654(6)
c (Å)	15.5323(9)	28.1709(15	13.4702(7)
α (º)	79.510(2)	90	90
β (º)	84.809(3)	90	108.661(2)
γ (°)	66.686(3)	90	90
Crystal size (mm)	0.257 x 0.183 x 0.129	0.296 x 0.028 x 0.025	0.606 x 0.190 x 0.131
V ($Å^3$)	1798.94(19)	5437.4(5)	2086.93(19)
Z	2	8	4
$Density_{calc.}$ ($Mg.m^{-3}$)	2.023	1.875	2.099
Absorption coefficient (mm^{-1})	6.940	5.991	7.780
F(000)	1056	3008	1256
θ range for data collection (°)	1.866 to 26.773	1.446 to 28.939	1.415 to 28.815
Index ranges	-13<=h<=13	-25<=h<=25	-14<=h<=20
	-15<=k<=15	-13<=k<=13	-14<=k<=14
	-19<=l<=19	-37<=l<=38	-18<=l<=14
Reflections measured	31440	97381	39153
Observed reflections [I > 2σ(I)]	6878	5847	5159
Independent reflections	7497	7127	5423
Data/restraints/parameter	7497 / 0 / 487	7127 / 0 / 361	5423 / 0 / 282
Goodness-of-fit on F^2	1.049	1.056	1.059
Observed R, wR^2	0.018, 0.047	0.028, 0.055	0.016, 0.036
R_{int}	0.025	0.058	0.0325

Table S2: *Selected bond lengths (Å) and angles (º) for* ***1****.*

Bond lengths (Å)		Bond angles (º)	
Re1-N9	2.207(3)	O15-Re1-N9	76.95(8)
Re1-O15	2.181(2)	C1-Re1-Cl2	173.03(10)
Re1-Cl2	2.4775(7)	C2-Re1-N9	172.6(1)
Re1-C1	1.905(3)	N5-Re2-C11	172.7(1)
Re1-C2	1.905(3)	C31-Re1-O15	171.83(11)
Re1-C31	1.902(3)	C2-Re1-C1	91.21(13)
Re2-N5	2.215(3)	C31-Re1-C1	90.46(13)
Re2-O14	2.1660(19)	C31-Re1-C2	85.34(13)
Re2-Cl1	2.4945(7)	O14-Re2-N5	76.87(8)
Re2-C11	1.915(3)	C12-Re2-O14	175.60(10)
Re2-C12	1.908(3)	C13-Re2-Cl1	174.75(9)
Re2-C13	1.903(3)	C12-Re2-C11	87.98(12)
C18-O9	1.224(3)	C13-Re2-C12	87.34(12)
C17-O15	1.273(4)	C13-Re2-C11	89.00(13)
C4-O14	1.269(4)		
C7-O5	1.227(5)		
C4-N7	1.381(5)		
C17-N3	1.383(3)		

Table S3: *Selected bond lengths (Å) and angles (º) for* ***2****.*

Bond lengths (Å)		Bond angles (º)	
Re1-N2	2.219(3)	Re1-N2	2.219(3)
Re1-N3	2.187(3)	Re1-N3	2.187(3)
Re1-Br1	2.6221(4)	Re1-Br1	2.6221(4)
Re1-C5	1.899(4)	Re1-C5	1.899(4)
Re1-C19	1.909(4)	Re1-C19	1.909(4)
Re1-C20	1.921(4)	Re1-C20	1.921(4)
C8-N3	1.291(4)	C8-N3	1.291(4)
C6-N2	1.446(4)	C6-N2	1.446(4)
C12-N3	1.449(4)	C12-N3	1.449(4)

Table S4: *Selected bond lengths (Å) and angles (º) for* ***3****.*

Bond Lengths (Å)		Bond Angles (º)	
Re1-N1	2.1852(18)	Re1-N1	2.1852(18)
Re1-N2	2.2453(17)	Re1-N2	2.2453(17)
Re1-Br1	2.6064(2)	Re1-Br1	2.6064(2)
Re1-C1	1.915(2)	Re1-C1	1.915(2)
Re1-C2	1.923(2)	Re1-C2	1.923(2)
Re1-C30	1.904(2)	Re1-C30	1.904(2)
C4-N1	1.288(3)	C4-N1	1.288(3)
C3-C4	1.452(3)	C3-C4	1.452(3)
C5-N1	1.429(3)	C5-N1	1.429(3)
C6-N3	1.401(3)	C6-N3	1.401(3)

In vitro anti-cancer studies

Cytotoxicity of metal complexes

The cytotoxicity and subsequent IC_{50} values of the three metal complexes were evaluated using the resazurin assay in three cell lines, namely the HeLa cervical cancer cell line (ATCC CCL-22), HCC70 basal triple negative breast cancer (TNBC) cell line (ATCC: CRL-2315), and a non-tumorigenic breast epithelial cell line MCF12A (ATCC: CRL-10782), according to Mbaba *et al*.[5, 6] Paclitaxel, a known chemotherapeutic compound for various cancers,[7] was also tested and used as a positive control. The cells were seeded at a density of 5000 cells/ well in a 96-well plate and allowed to attach overnight at 37 ^{o}C and 9% CO_2. The cells were then treated for 96 hr with the various complexes at a concentration range of 15.63 to 500.00 µM or 2% (*v/v*) dimethyl sulphoxide (DMSO) as a vehicle control or paclitaxel (0.16 to 500 nM) at 37 ^{o}C and 9% CO_2. After a 96-hr incubation, 20 µL of 0.54 nM Resazurin solution was added to the wells. The cells were then incubated for 2-4 hours at 37 ^{o}C in a 9% CO2 incubator, and fluorescence readings were obtained on a Spectramax spectrophotometer (excitation and emission wavelengths set at 560 nm and 590 nm, respectively). The experiment was performed in triplicate, and the data were analysed using GraphPad Prism Inc. (USA), with half-maximal inhibitory concentration (IC_{50} values) determined by non-linear regression.

Clonogenic assay to determine the effect of complex 2 on long-term survival

HCC1806 breast cancer cells (ATCC CRL-2335) were seeded at a density of 1000 cells/well in a 6-well plate and allowed to adhere overnight in an incubator at 37 ^{o}C and 9% CO_2. The cells were then treated with either complex **2** (5 µM, 25 µM or 125 µM) or DMSO [0.005, 0.025 or 0.125% (*w/v*)]). Thereafter, the culture medium was replaced every 2 days for a duration of 10 days. The cells were allowed to grow until individual colonies were visible. On the 10th day, the media was removed and the cells were washed three times with PBS. The cells were fixed in 1 mL of methanol: acetic acid (3:1) for 5 minutes; air dried and stained with 1 mL 5% (*w/v*) crystal violet in methanol overnight. Thereafter, the wells were washed 3 times in PBS and rinsed in ddH_2O. The plates were air dried, and images were obtained using the ChemiDoc™-XRS (BioRad, USA). The contents of the wells were solubilized in 1 mL 1x acetic acid and absorbance read in triplicate at 595 nm on the SynergyMx spectrophotometer. The experiment was performed in biological duplicate and technical triplicate, and the data were analysed using GraphPad Prism Inc, (USA).[7 8]

DNA binding studies

Ethidium bromide competition using agarose gel electrophoresis

The ability of the metal compounds to competitively bind to genomic DNA (gDNA) isolated from HCC70 cells to displace ethidium bromide (EtBr) was assessed using agarose gel electrophoresis (AGE).[9] AGE was performed after incubating complex **2** (50 µM or 200 µM), DMSO [0.2% (*v/v*)] or cisplatin (200 µM) with 100 ng of gDNA for 4 hours at 37°C in a total volume of 20 µL. Thereafter, 10 µL of reaction mixture and 2 µL of 6x loading dye were loaded onto a 0.6% (w/v) agarose gel containing 0.5 µgg/mL EtBr. The agarose gel was electrophoresed at 90 V in 1*x* Tris-acetic acid EDTA [TAE (40 mM Tris-acetate, 1 mM EDTA)] for 45 minutes. Visualisation of the resulting bands was detected using a ChemiDoc XRS System (Bio-Rad Laboratories) with Image Lab Software (Bio-Rad Laboratories).[10]

Methylene blue DNA competition binding study

A methylene blue DNA competition binding assay was performed to determine whether complex **2** can compete with methylene blue to bind to calf thymus DNA by intercalation .[5, 11, 12] A 15 µg/mL solution of methylene blue dye, 100 ng calf thymus DNA (*ct*DNA), complex 2 (50 µM or 200 µM) and nuclease-free water, with a final 100 µL reaction volume, was added to a clear-bottomed black 96-well plate and incubated at room temperature in the dark for 10

minutes. The fluorescence was then measured in 5 nM wavelength intervals at an excitation wavelength of 665 nM and an emission wavelength range of 650 to 690 nM on a Spectramax spectrophotometer.[5] The experiment was performed in triplicate, and the data were analysed using GraphPad Prism Inc. (USA).

ctDNA UV-Vis spectrophotometric titration

The DNA binding susceptibility of **2** was further explored towards *ct*DNA in phosphate buffer solution (PBS). This study was carried out at the physiological temperature of 37°C. The UV absorbance ratio at 260 and 280 nm of a prepared solution of CT-DNA was 1.8:1, indicating that the DNA was free of bound proteins.[13] The metal complex and DNA solutions were incubated for one day at 25°C before UV-Vis measurements were undertaken. The Wolfe-Schimmer was used to calculate the intrinsic binding constant:[14]

$$[DNA]/(\varepsilon_a - \varepsilon_f) = [DNA]/(\varepsilon_b - \varepsilon_f) + 1/K_b(\varepsilon_b - \varepsilon_f)$$

In the equation, the [DNA] is the concentration of DNA, ε_b is the extinction coefficient of the complex, ε_a is the extinction coefficient of the absorption band at the given [DNA] (A_{obs}/[complex]), ε_f is the extinction coefficient of the complex free in solution, and when fully bound to DNA. A linear correlation of $[DNA]/(\varepsilon_a - \varepsilon_f)$ versus [DNA] gives a slope of $1/(\varepsilon_a - \varepsilon_f)$ and a *y*-intercept equal to $1/K_b(\varepsilon_b - \varepsilon_f)$. The intrinsic binding constant, K_b can be obtained using the slope to intercept ratio.

Topoisomerase I inhibition study

In order to determine whether metal complex **2** affected the ability of the enzyme topoisomerase I (Topo I) to relax supercoiled DNA, a Topo I inhibition study was performed according to the method adapted from Kadioglu.[15] A reaction mixture containing 215 ng plasmid pcDNA, 1*x* reaction buffer (10 mM Tris-HCl pH 7.5, 10 mM KCl, 2 mM $MgCl_2$, 0.1 mM DTT, 0.02 mM EDTA and 6 µg/mL BSA), 1 unit of Topo 1 enzyme and complex 2 (50 µM or 200 µM), made up to a total reaction volume of 10 µL in nuclease-free water, was incubated at room temperature for 15 minutes. The reaction mixture and 2 µL of 6x loading dye were loaded onto a 0.6% (*v/v*) agarose gel without ethidium bromide (EtBr) and electrophoresed in TAE buffer at a voltage of 90 V for 35 minutes. Various controls were also loaded onto the 0.6% (*w/v*) agarose gel, which included a digested plasmid (digested with 5 units Hind III overnight, used to visualize a linear digested DNA fragment), supercoiled pcDNA plasmid (without Topo I) and untreated Topo I and plasmid (uninhibited control). Once the agarose gel was electrophoresed, it was then stained with 50 µg/mL of EtBr for 20 min and washed twice with ddH_2O. The resulting bands were then visualized under UV light with a Digital Imaging System (BIO-RAD, USA).

Alkaline Comet assay

The alkaline comet assay adapted from Olive and Banath (2006) was performed for metal complex **2**. HCC70 TNBC cells were seeded at a density of 2×10^5 cells/well in a 12-well plate.[15] The cells were allowed to attach overnight at 37 °C and 9% CO_2 and then treated with a vehicle control (0.04% (*v/v*) DMSO) or complex **2** (20 µM or 40 µM) for 1 hr at 37 °C and 9% CO_2. Thereafter, the cells were trypsinized and centrifuged at 1600 rpm for 5 minutes. The pelleted cells were resuspended in cold PBS and the cell density was adjusted to 2×10^4 cells/mL in PBS. The cells were suspended in 1% (*w/v*) low gelling temperature agarose and placed on slides pre-coated with 1% (*w/v*) low gelling temperature agarose and allowed to set for 2 minutes. The cells were lysed overnight in the dark at 4 °C in A1 lysis buffer (1.2 M NaCl; 100 mM Na_2EDTA; 0.1% (*w/v*) sodium lauryl sarcosinate; 0.26 M NaOH). The lysis buffer was removed, and the slides were washed three times for 20 minutes in A2 rinse and electrophoresis buffer (0.03 M NaOH, 2 mM Na_2EDTA). The slides were then electrophoresed in A2 rinse and electrophoresis buffer for 25 minutes at 20 V and 40 mA. The electrophoresis buffer was removed, and the slides were washed with ddH_2O and stained with 10 µg/mL propidium iodide (PI) for 20 minutes. Excess stain was removed by rinsing the slides in ddH_2O. The comets under 20x magnification were then visualised using an Olympus BX43 optical fluorescence microscope, and

100 comet images were taken per treatment using an Olympus DP74 digital camera with CellSens Entry Software. The comets were visualised using a U-MWG wide green filter cube with an excitation wavelength of 510 nM, an emission wavelength of 590 nM and a beamsplitter wavelength of 570 nM. The captured comets were analysed using an Image J Plugin, OpenComet (Gyrori et al., 2014), allowing for measurement of DNA damage according to Olive moment [Tail DNA% % *x* (length of tail – length of head)].[16] The data were analysed using GraphPad Prism Inc. (USA) to generate box and whisker plots, and statistical analysis was carried out using a Mann-Whitney test.

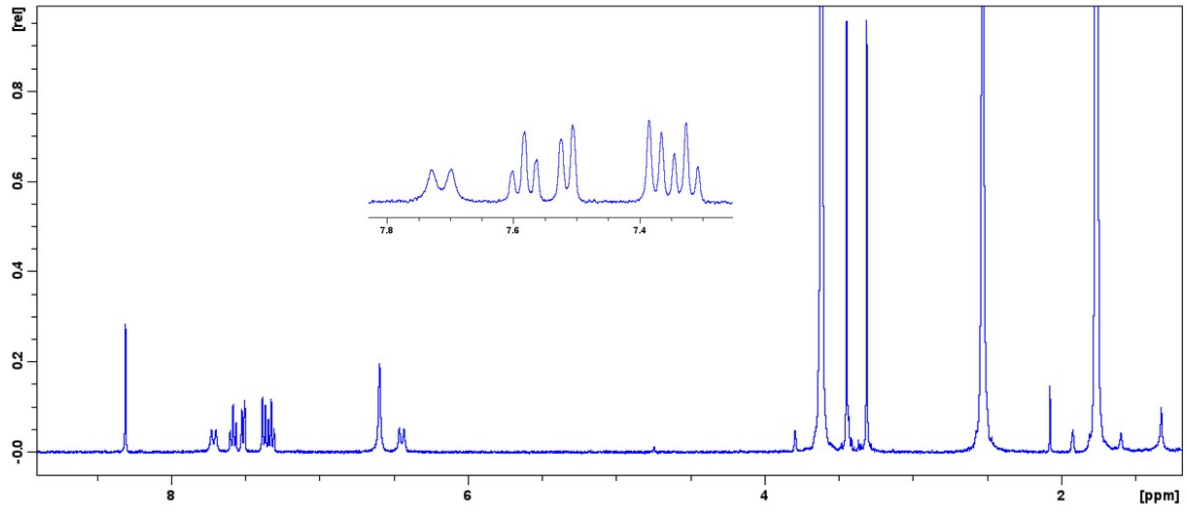

Figure S7: *^{1}H NMR spectrum of fac-[Re(CO)$_3$(uramb)Br]. Inset shows aromatic protons 6.43 – 7.73 ppm.*

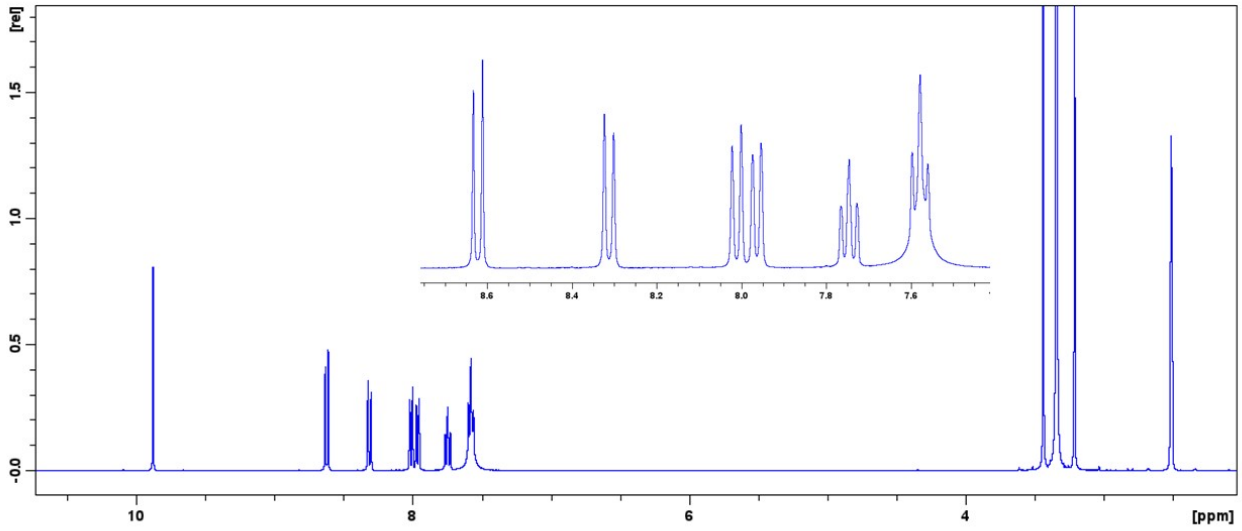

Figure S8: *^{1}H NMR spectrum of fac-[Re(CO)$_3$(urqn)Br]. Inset shows aromatic protons between 7.49 – 8.70 ppm.*

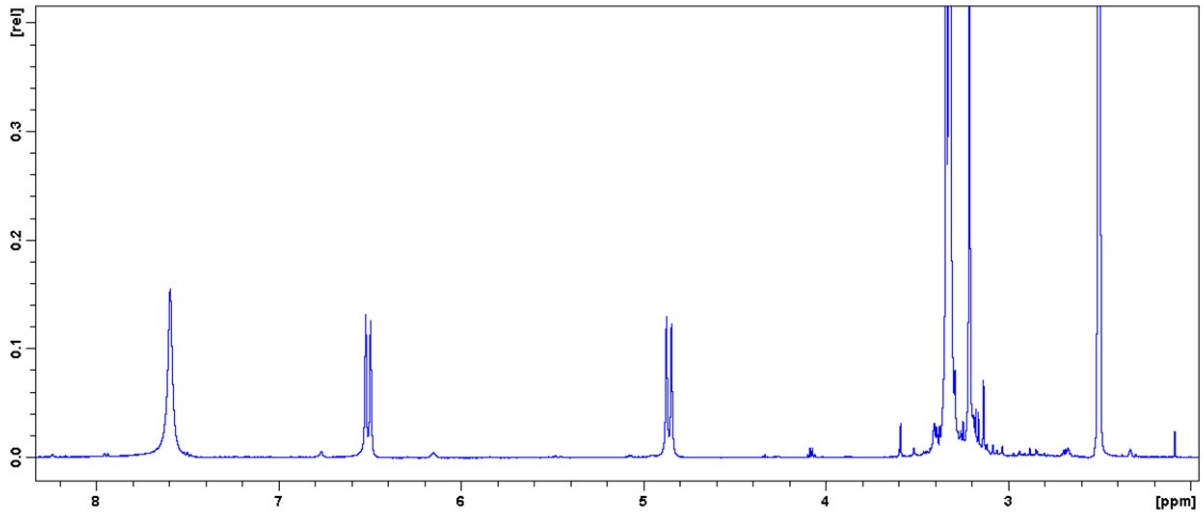

Figure S9: *^{1}H NMR spectrum of fac-[Re(CO)$_3$(urda)Cl].*

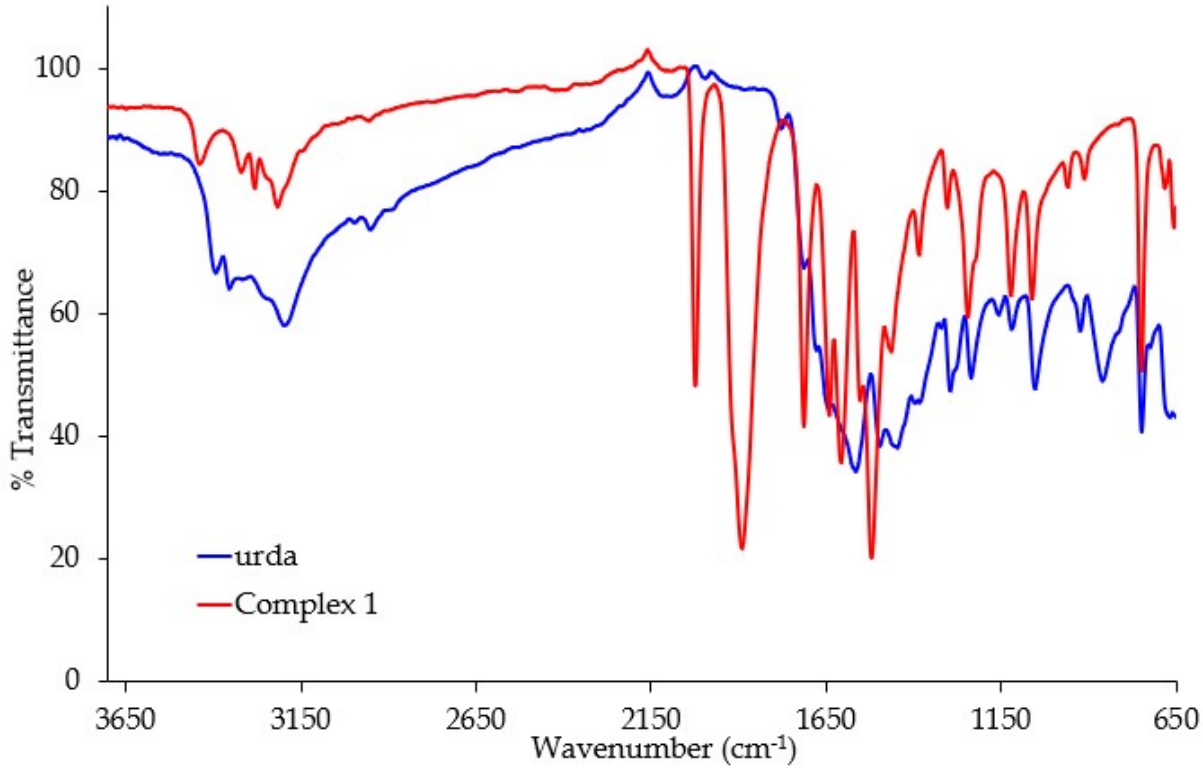

Figure S10: *IR spectrum of fac-[Re(CO)$_3$(urda)Cl] and its free-ligand urda.*

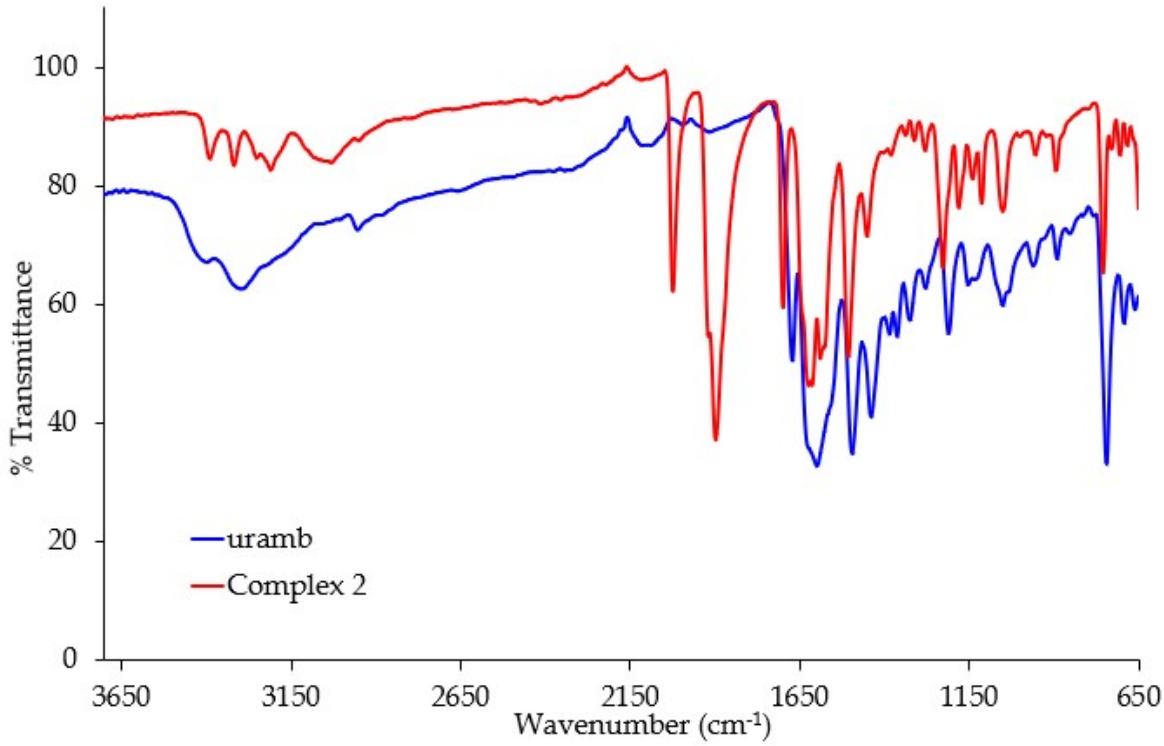

Figure S11: *Overlay IR spectra of fac-[Re(CO)$_3$(uramb)Br] and its free ligand, uramb.*

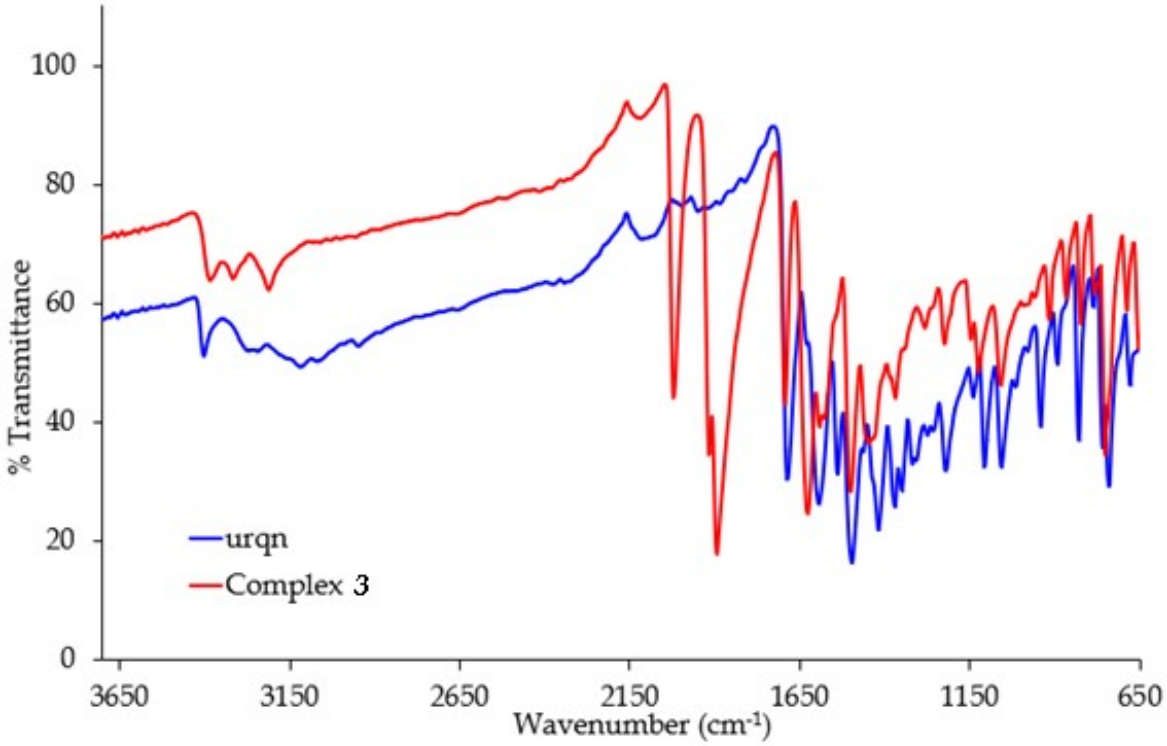

Figure S12: *Overlay IR spectra of fac-[Re(CO)$_3$(urqn)Br] and its free ligand, urqn.*

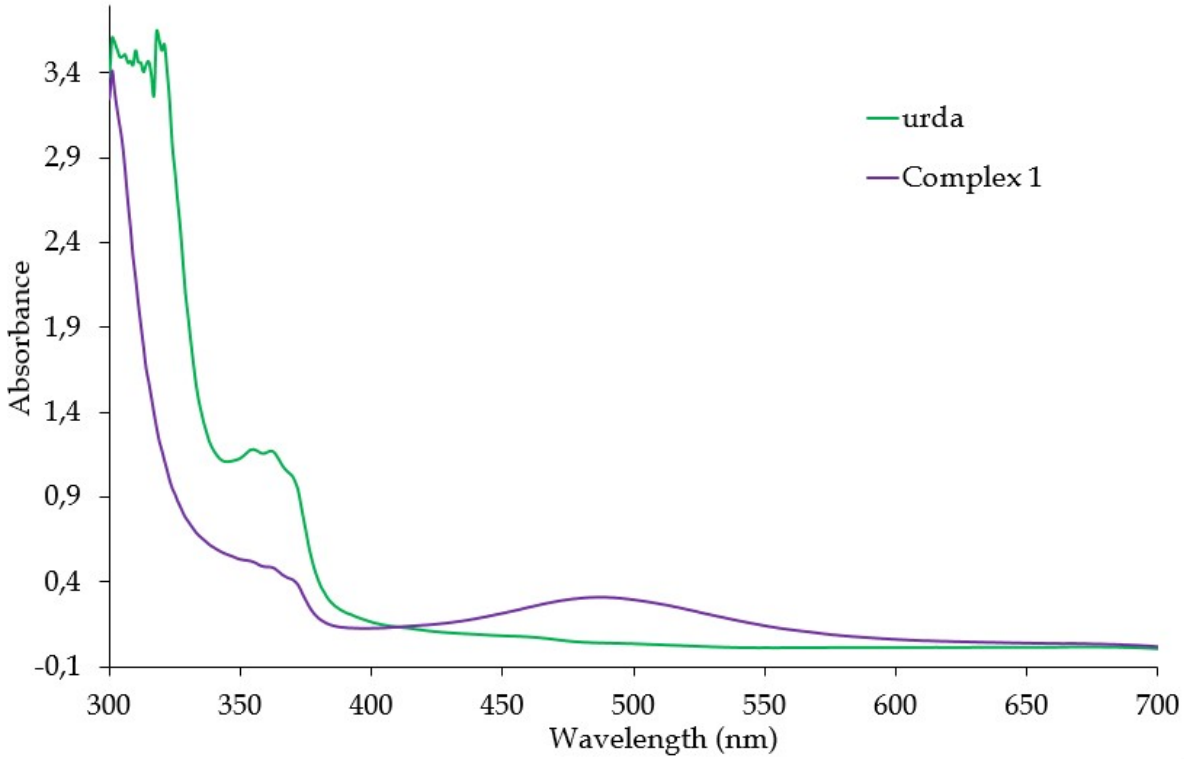

Figure S13: *Overlay UV-Vis spectra of fac-[Re(CO)$_3$(urda)Cl] and its free ligand, urda.*

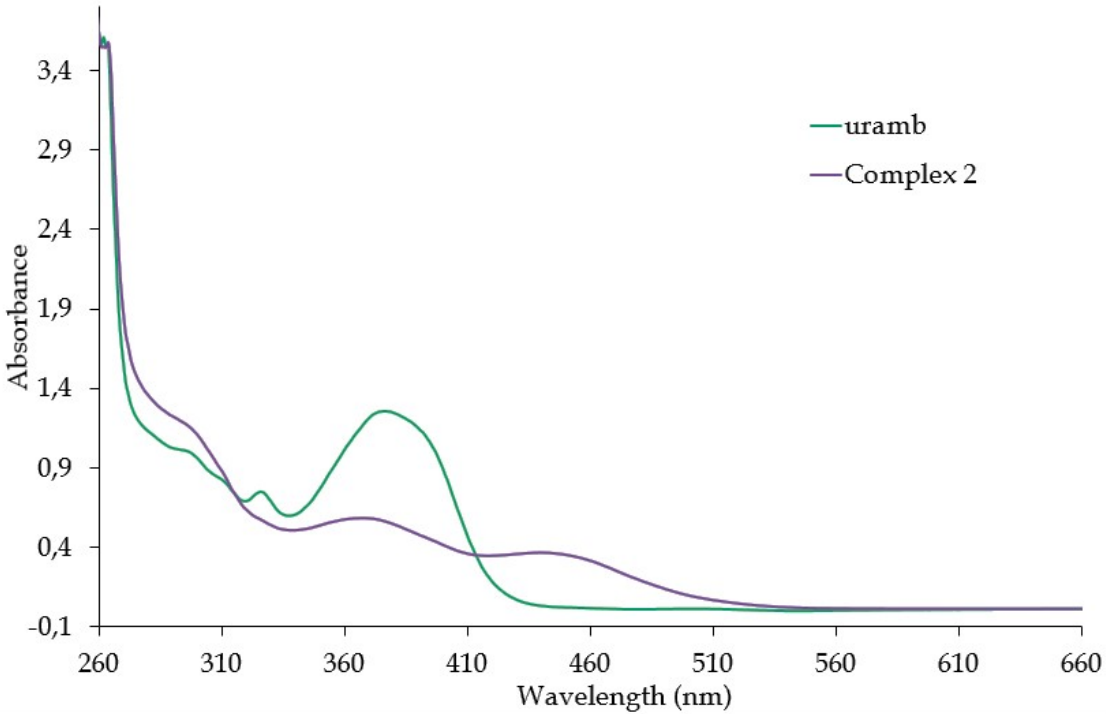

Figure S14: *Overlay UV-Vis spectra of fac-[Re(CO)$_3$(uramb)Br] and its free ligand, uramb.*

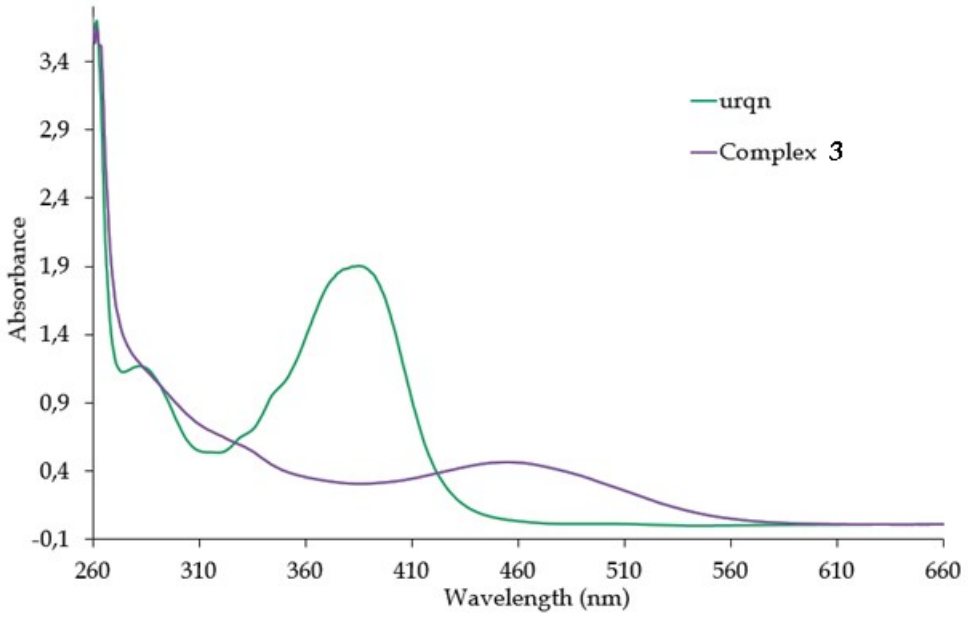

Figure S15: *Overlay UV-Vis spectra of fac-[Re(CO)$_3$(urqn)Br] and its free ligand, urqn.*

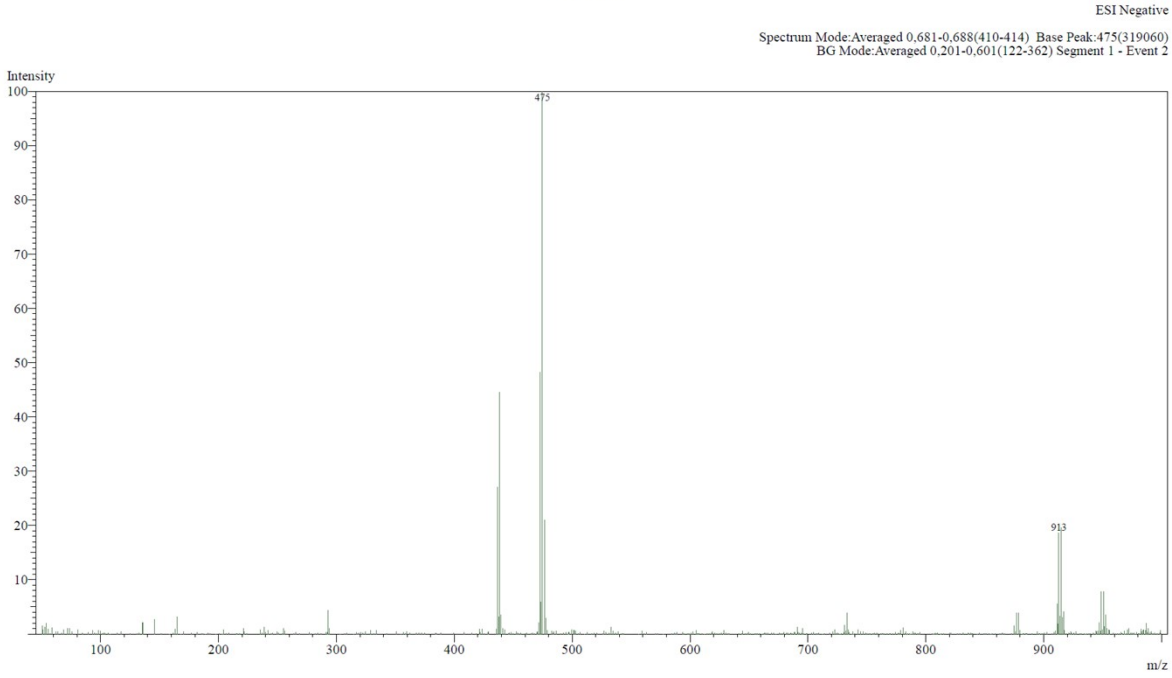

Figure S16: *MS spectrum of fac-[Re(CO)$_3$(urda)Cl].*

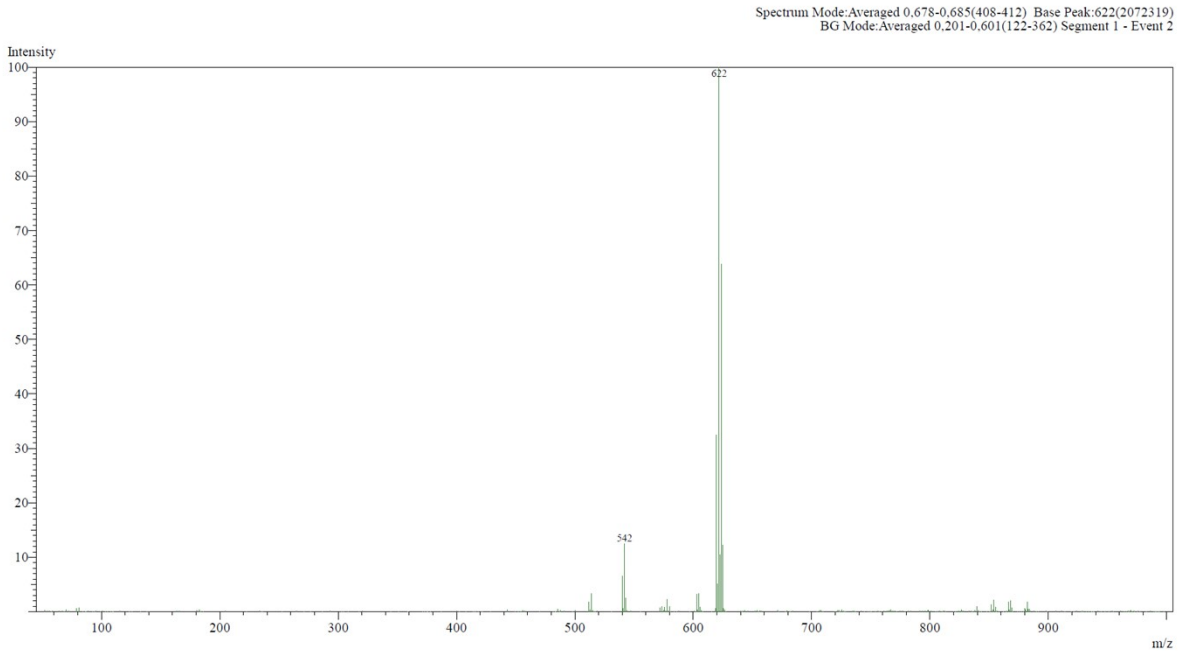

Figure S17: *MS spectrum of fac-[Re(CO)$_3$(uramb)Br].*

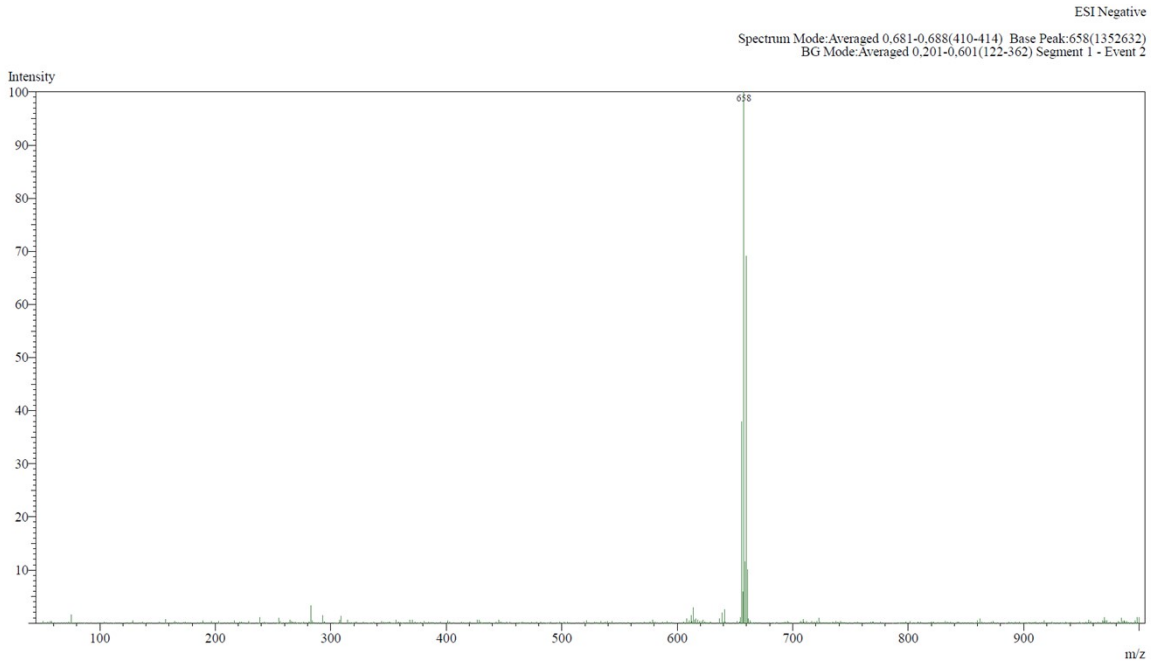

Figure S18: *MS spectrum of fac-[Re(CO)$_3$(urqn)Br]*

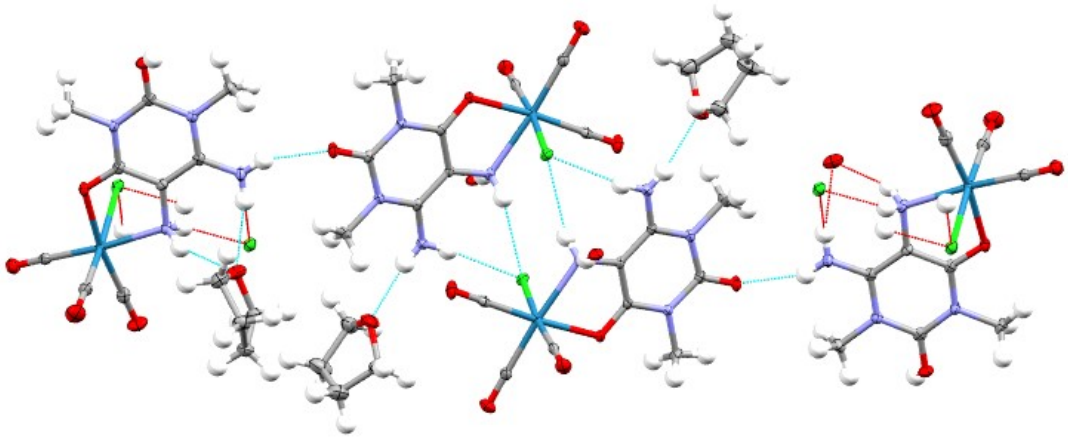

Figure S19: *A perspective of the crystal lattice of **1** illustrating the hydrogen-bonding interactions between the molecules.*

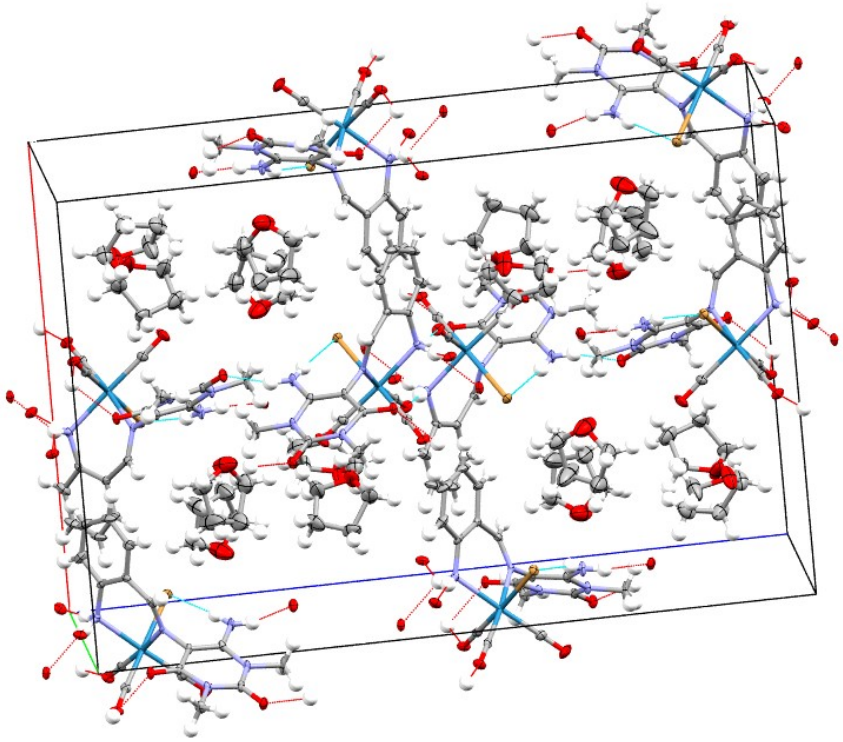

Figure S20: *The asymmetric unit cell of **2** showing hydrogen-bonding interactions between the packed molecules.*

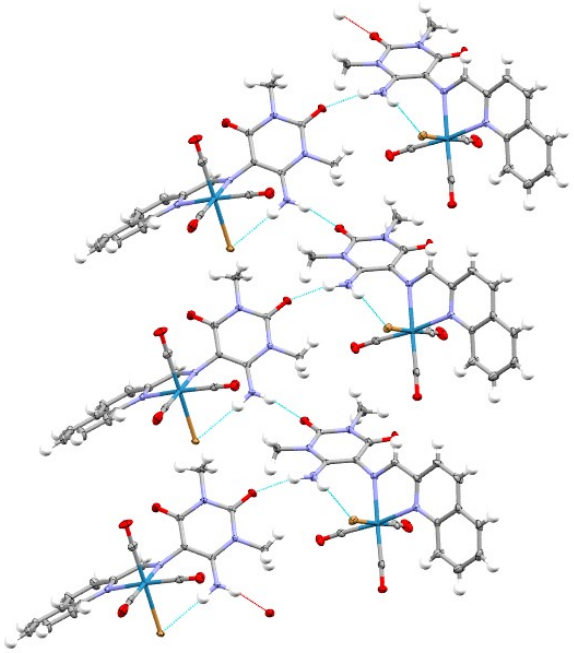

Figure S21: *A perspective of the crystal lattice of **3** showing the stabilizing hydrogen-bonding interactions.*

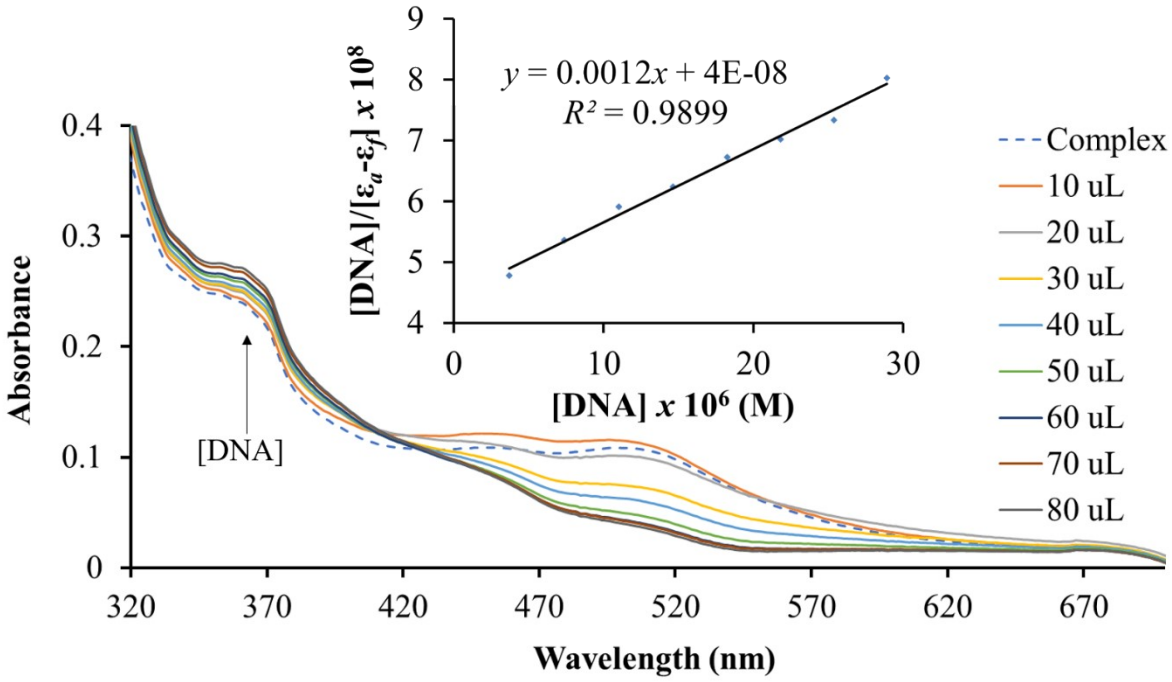

Figure S22: *Overlay UV–Vis spectra of **2** obtained from its titration against subsequent additions of CT-DNA. The arrow shows the increasing intensity of the intra-ligand electronic transition at 363 nm. The inserted graph shows the plot of [DNA]/($\varepsilon_a - \varepsilon_f$) x 10^8 vs [DNA] x 10^6.*

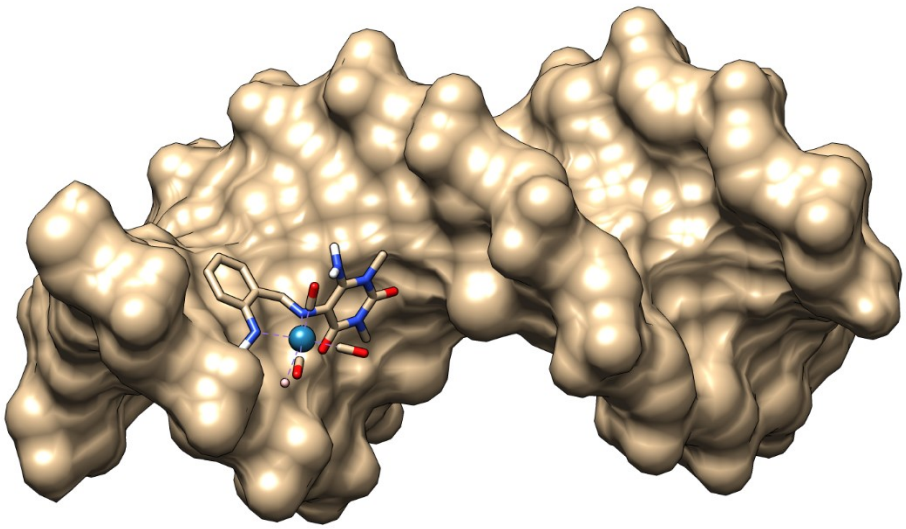

Figure S23: *A perspective view of the minimum energy conformer of the **2**-DNA adduct, where the metal complex displays DNA groove-binding.*

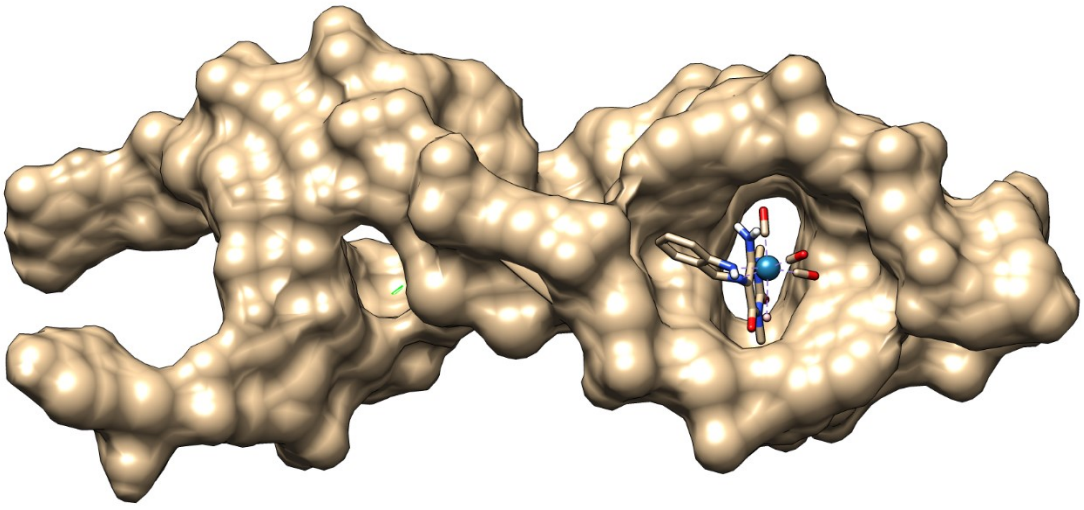

Figure S24: *A perspective view of the minimum energy conformer of the **2**-DNA adduct, where the metal complex displays DNA intercalation.*

Computational studies

Simultaneous molecular optimisation and frequency calculation were performed at the Density Functional Theory level using the resources of the South African Centre for High Performance Computing (CHPC). Firstly, the crystal structure of **2** was amended by deleting the solvent molecules of recrystallisation, and then the resultant structure was used as a starting conformer. Thereafter, the input file was prepared using the Gaussian 09W software package. The 6-311G^{++} (*d*, *p*) basis set was applied to all the non-metals, while the metal centre had a Los Alamos National Laboratory 2 double-ζ (LANL2DZ) basis set.[17] Data validation was established based on the fact that the simulated infrared spectrum of **2** had no constrained vibrations with negative energies. The latter was also corroborated by the good comparison between the optimised and experimental conformers of **2**, see **Figure S25**.

AutoDock 4.2.6 was utilised to perform the molecular docking studies on a personal laptop computer.[18] As the parameters of the rhenium atom are not embedded within the software, its calculated parameters were attained with the assistance of the support services *via* the website https://autodock.scripps.edu/ (accessed: 22/08/2025). To evaluate the optimised conformer of **2**'s tandem DNA binding capabilities, DNA crystal structures with the following Protein Data Bank Identifications (PDB IDs): 4E1U and 425d were used, where the latter is typically used for groove-binding interrogations, while the former is preferred for investigating DNA intercalation interactions of small molecules.[19-21]

Prior to the simulations, the DNA receptor molecules had to be prepared by the removal of all heteroatoms and water molecules of recrystallisation. Subsequently, Gasteiger charges were added to the different conformers. For the starting conformers generated from 425d, a grid box dimension of 110 x 66 x 68 with a spacing of 0.375 Å was used, whereas for 4E1U, the grid box dimension and spacing were 108 x 88 x 126 and 0.45 Å, respectively. Both output files were expressed in the Lamarckian format, and the search parameters were set to the genetic algorithm. Visualisations were captured with the aid of BIOVIA Discovery Studio 2025.

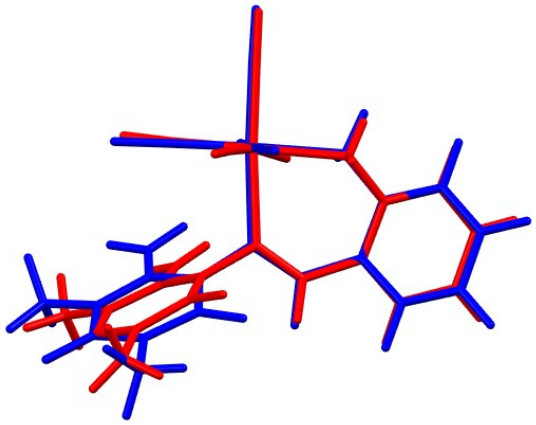

Figure S25: *Overlay structures of **2**, where the crystal structure is the red conformer and the optimized structure is the blue conformer. Root-mean-square deviation distances (RMSDs) of 0.7918 Å*

References:

1. R. H. Blessing, *Acta Crystallographica Section A: Foundations of Crystallography*, 1995, **51**, 33-38.
2. G. M. Sheldrick, *Acta Crystallographica Section A: Foundations of Crystallography*, 2008, **64**, 112-122.
3. G. Sheldrick, *University of Gottingen, Germany*, 2018.
4. L. J. Farrugia, *Journal of Applied Crystallography*, 2012, **45**, 849-854.
5. M. Mbaba, L. M. K. Dingle, D. Cash, J.-A. d. l. Mare, D. Laming, D. Taylor, H. C. Hoppe, A. L. Edkins and S. D. Khanye, *European Journal of Medicinal Chemistry*, 2020, **187**, 111924.
6. C. Davison, S. Abdullah, C. J. Smit, P. Dlamini, I. N. Booysen and J.-A. d. l. Mare, *Chemico-Biological Interactions*, 2025, **406**, 111351.
7. N. A. P. Franken, H. M. Rodermond, J. Stap, J. Haveman and C. van Bree, *Nature Protocols*, 2006, **1**, 2315-2319.
8. L. Gutiérrez, G. Stepien, L. Gutiérrez, M. Pérez-Hernández, J. Pardo, J. Pardo, V. Grazú and J. M. de la Fuente, in *Comprehensive Medicinal Chemistry III*, eds. S. Chackalamannil, D. Rotella and S. E. Ward, Elsevier, Oxford, 2017, DOI: https://doi.org/10.1016/B978-0-12-409547-2.12292-9, pp. 264-295.
9. L. Gramni, N. Vukea, A. Chakraborty, W. J. Samson, L. M. K. Dingle, B. Xulu, J.-A. de la Mare, A. L. Edkins and I. N. Booysen, *Inorganica Chimica Acta*, 2019, **492**, 98-107.
10. C. A. Schneider, W. S. Rasband and K. W. Eliceiri, *Nature Methods*, 2012, **9**, 671-675.
11. W.-Y. Li, J.-G. Xu and X.-W. He, *Analytical Letters*, 2000, **33**, 2453-2464.
12. P. O. Vardevanyan, A. P. Antonyan, M. A. Parsadanyan, M. A. Shahinyan and L. A. Hambardzumyan, *Journal of Applied Spectroscopy*, 2013, **80**, 595-599.
13. M. B. Ismail, I. N. Booysen, M. P. Akerman and C. Grimmer, *Journal of Organometallic Chemistry*, 2017, **833**, 18-27.
14. S. Maikoo, A. Chakraborty, N. Vukea, L. M. K. Dingle, W. J. Samson, J.-A. de la Mare, A. L. Edkins and I. N. Booysen, *Journal of Biomolecular Structure and Dynamics*, 2021, **39**, 4077-4088.
15. O. Kadioglu, A. Chan, A. Cong Ling Qiu, V. K. W. Wong, V. Colligs, S. Wecklein, H. Freund-Henni Rached, T. Efferth and W.-L. W. Hsiao, *Frontiers in Pharmacology*, 2017, **8**.
16. B. M. Gyori, G. Venkatachalam, P. S. Thiagarajan, D. Hsu and M. V. Clement, *Redox Biol*, 2014, **2**, 457-465.
17. M. B. Ismail, I. N. Booysen and M. P. J. I. C. A. Akerman, *Inorganica Chimica Acta*, 2018, **477**, 257-269.
18. G. M. Morris, R. Huey, W. Lindstrom, M. F. Sanner, R. K. Belew, D. S. Goodsell and A. J. Olson, *J Comput Chem*, 2009, **30**, 2785-2791.
19. S. Sookai, M. Akerman, M. Færch, Y. Sayed and O. Q. Munro, *European Journal of Medicinal Chemistry*, 2025, **287**, 117330.
20. H. Song, J. T. Kaiser and J. K. Barton, *Nature Chemistry*, 2012, **4**, 615-620.
21. H. Rozenberg, D. Rabinovich, F. Frolow, R. S. Hegde and Z. Shakked, *Proceedings of the National Academy of Sciences*, 1998, **95**, 15194-15199.